Target recognition and visual maps in the thalamus of achiasmatic dogs

Robert W. Williams*, Dale Hogan* & Preston E. Garraghty†

* Department of Anatomy and Neurobiology, University of Tennessee School of Medicine, 855 Monroe Avenue, Memphis, Tennessee 38163, USA
† Program in Neural Science, Department of Psychology, Indiana University, Bloomington, Indiana 47405, USA

VISION is dependent on ordered neuronal representations or maps of visual space. These maps depend on precise connections between retinal axons and their targets cells. In mammals, nerve fibres from right and left eyes produce congruent maps of contralateral visual space in adjacent layers of the lateral geniculate nucleus (LGN)[1]. We have identified an autosomal recessive mutation in Belgian sheepdogs[2,3] that eliminates the optic chiasm. In these mutants, all retinal axons project into the ipsilateral optic tract, including those originating in the nasal hemiretina that normally cross midline. These animals exhibit a pronounced horizontal nystagmus[4,5]. The abnormal ipsilaterally directed nasal fibres innervate the LGN as if they had successfully crossed the midline, terminating in the appropriate layer of the nucleus. As a consequence, the LGN contains non-congruent, mirror-image maps of visual space in adjacent layers. These results show that there is a robust affinity between nasal and temporal retinal axons and specific LGN layers even when all retinal axons originate from a single eye.

Other than the elimination of the optic chiasm, no other midline abnormalities are evident in the mutant dogs. In seven of eight cases, the crossed component of the optic chiasm is absent (Fig. 1). The optic nerves fail to approach midline, and maintain a separation of 5–8 mm as they enter the thalamus. In one animal (M2), a small contralateral retinal projection was apparent (D.H. and R.W., unpublished results).

The shape and lamination of the LGN in the normal dog resembles that of other carnivores. In comparison to the cat, the central field representation in the dog is positioned more rostrally, and the caudal, vertically oriented limb of the nucleus is more prominent (Fig. 2*a*)[1,6]. The LGN of mutant dogs closely resembles that of normal dogs in overall size, shape, and cellular composition (Fig. 2*b*). A prominent interlaminar zone separates layers A and A1 through the central part of the nucleus of mutants. In contrast to normal dogs, the interlaminar zone does not extend into the rostromedial part of the nucleus. In this area, which represents central visual fields, layers A and A1 are fused (Fig. 2*b*, *c*). Upper visual fields are located caudomedially, and lower visual fields are located rostrolaterally in the LGN of both normal and mutant dogs. The monocular segment of the visual field of normal animals is situated in the dorsocaudal limb of the LGN. As in other carnivores[7], receptive fields recorded from neighbouring segments of layers A and A1 in normal dogs view the same area of contralateral visual space.

In mutants, as in normal dogs, visual stimuli in the contralateral field evoked vigorous responses in layer A1 (Fig. 3). This relatively small, normal ipsilateral temporal projection is unperturbed by the aberrant ipsilateral input of nasal retina to neighbouring layer A. In each mutant, the entire aberrant nasal projection establishes functional connections throughout ipsilateral layer A. These aberrant ipsilateral fields extended to 90–100° in azimuth and included the region occupied by the contralateral monocular segment of layer A in normal dogs. The misconnection of the nasal retina leads to a severe misalignment of visual maps in layers A and A1. Within a large central segment of the LGN, we repeatedly recorded abrupt reversals in receptive field azimuth (Fig. 3, curved arrows). The size of the reversals varied systematically with the mediolateral position of the penetration. In medial parts of the LGN, small jumps in azimuth were recorded. In more lateral parts of the LGN, large jumps in azimuth were observed (Fig. 3). These reversals across the vertical meridian representations occurred as the electrode crossed the border between A and A1.

The achiasmatic Belgian sheepdog is the first mutant vertebrate in which the size of the ipsilateral retinal projection is increased. Interestingly, achiasmatic humans have also been described recently[8]. The achiasmatic mutation has an effect opposite to that produced by albinism, which increases the size of the contralateral projection. However, the achiasmatic mutation is not a simple anti-albino. In albinism, the line of decussation is shifted towards the temporal edge of the retina and there is invariably a residual uncrossed projection from the far temporal retina[9–13]. In contrast, in achiasmatic dogs, the phenotype is more extreme because the much larger nasal projection is misrouted and there is usually no residual crossed projection. Although the misrouting of axons in mutant dogs has an opposite pattern to that seen in albinos, the fundamental mapping errors are reminiscent of those observed in the LGN of Siamese cats and albino ferrets[14–17] (Fig. 4*b*, *c*).

The novel pattern of misrouting of retinal fibres in achiasmatic mutants provides a challenging natural experiment that can be used to study processes responsible for generating LGN lamina-

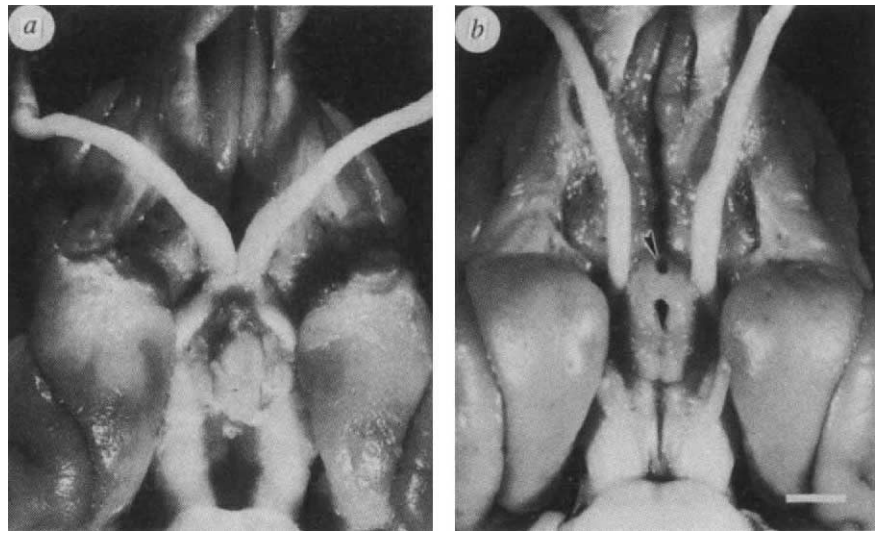

FIG. 1 Ventral views of Belgian sheepdog brains showing *a*, the normal, and *b*, the mutant achiasmatic phenotypes (case M3). *a*, In the normal dog, the two optic nerves meet at midline, and about 80% of the retinal fibres from each nerve cross midline to enter the contralateral optic tract. *b*, In most mutants, the chiasm is eliminated entirely, and all fibres extend into the ipsilateral tract. The minimum distance separating the two retinal projections is ~5 mm. The arrowhead points to the lamina terminalis of case M3. This structure is normally covered ventrally by the optic chiasm. The pituitary has been removed in *b*, exposing the floor of the third ventricle at the midline. Scale bar, 5 mm.

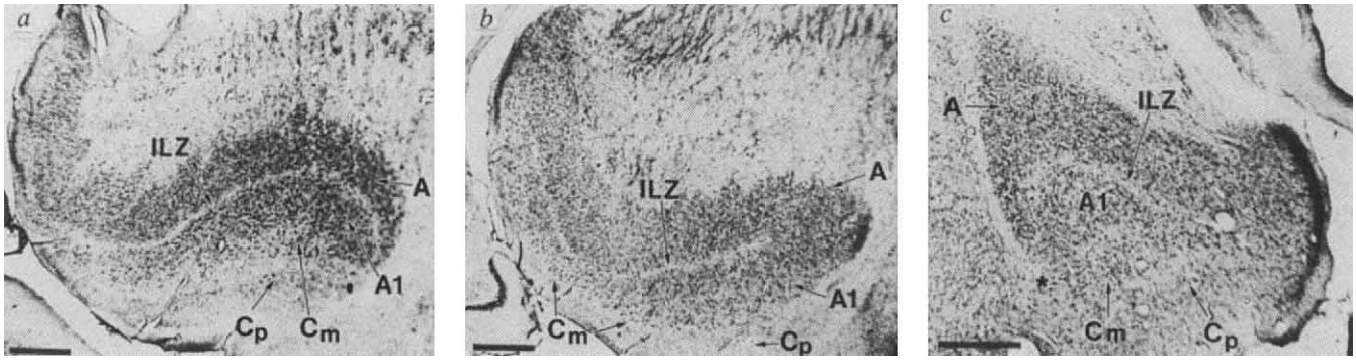

FIG. 2 Lamination of the LGN in normal and achiasmatic mutant dogs. *a*, In this parasagittal plane, the A layer of the LGN of a normal dog appears S-shaped, with its caudal (left) and rostral (right) parts wrapping dorsally and ventrally, respectively. Layer A1 is separated from layer A by a cell-sparse interlaminar zone (ILZ). Note that in the caudal part of the LGN, layer A1 is normally situated caudal to layer A. The magnocellular C layer (C_m) follows the S-shape caudally and extends beneath both layers A and A1 in the rostral, binocular portion of the nucleus. Unlike the situation in cats, there is no interlaminar zone between layer C_m and layer A1 in the dog[6]. The parvicellular C layers (C_p) are located in the most caudal and ventral portions of the LGN. These layers are thinner than C_m and are separated from C_m by a narrow interlaminar zone. *b*, Parasagittal section through the LGN of mutant M3, about 0.5 mm medial to that of the normal dog shown in *A*. The nucleus is similar in overall shape and size to that of normal dogs. However, the interlaminar zone between layers A and A1 is only present in the mid- and caudal portions of the nucleus. In the rostral LGN, layers A and A1 are tightly apposed or fused in mutants. Similar lamination defects may be present in the C layers, but they are not obvious in Nissl-stained material. Cell size does not differ from that of normal animals. *c*, Photomicrograph of a coronal section through the LGN of mutant M1. Fusion of A and A1 is evident on the medial (left) side of the nucleus. The asterisk indicates the location of an electrolytic lesion made along penetration P6 at the junction of A1 with C_m, and corresponds in position to the double asterisk in Fig. 3. Scale bar on each photomicrograph represents 1 mm.

tion and visual maps (Fig. 4). In the achiasmatic dog, a single retina innervates a structure that normally receives input from two retinae. A single input that projects to a single nucleus might be expected to produce a single map in an unlaminated nucleus. This is the pattern found in the LGN after unilateral enucleation early in development[18,20] (Fig. 4*d*) and also found normally in another retinal target—the superior colliculus[21]. In fact, the LGN of mutants is laminated and nasal retinal fibres terminate in ipsilateral layer A with the same anatomical polarity normally seen in the contralateral LGN—the central nasal part of retina projects into the rostral and medial part of the LGN and the peripheral nasal part of the retina projects into the caudal and lateral part of the nucleus. As these fibres have not crossed midline, the physiological polarity of the projection is reversed, both

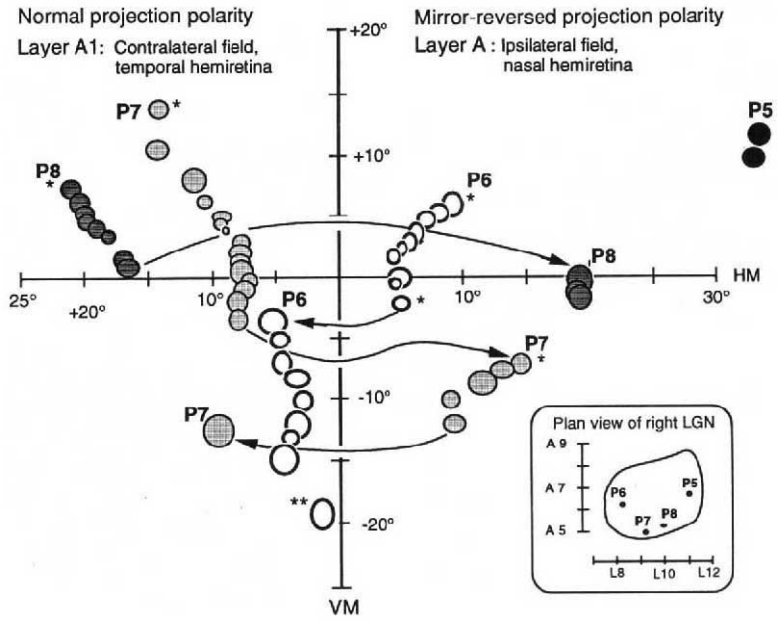

FIG. 3 Receptive field discontinuities in the achiasmatic mutant. These data are taken from case M1. Note the large receptive field discontinuities (long curved arrows) along each of three penetrations through the LGN (P6–P8). The large, nearly symmetrical shifts in azimuth across the vertical meridian representation (VM) is larger in the more lateral penetrations (P7 and P8). Electrolytic lesions (*) were used to verify that the jumps occurred at the borders between layers. Double asterisk marks a lesion along P6 that is also marked in Fig. 2*c*. Penetrations P7 and P8 were so far caudal in the LGN that the electrode initially traversed layer A1 before finally entering layer A. In contrast, more rostral penetrations initially traversed layer A and then passed into A1. The most lateral penetration (P5) extended through the far peripheral representation that would represent the monocular segment of the LGN in a normal dog. The progression of fields from high to low elevation is normal, and is caused by the dorsoventral orientation of geniculate layers. Small inset is a schematic plan view of the four electrode penetrations. HM, approximate horizontal meridian representation; VM, approximate vertical meridian representation.

METHODS. We recorded from three mutant dogs ranging in age from 3 months to 1 year (M1, M2 and M3; 5–22 kg). As controls, we recorded from one behaviourally normal Belgian sheepdog and three normal adult mongrels (8–24 kg). Dogs were sedated with ketamine hydrochloride (7 mg kg^{-1}) and xylazine (0.4 mg kg^{-1}). Anaesthesia was induced with sodium pentobarbital (15–20 mg kg^{-1}). During the course of the experiments, anaesthesia was maintained by infusing sodium pentobarbital (3 mg kg^{-1} h^{-1}). Paralytic agents were not used. Heart rate was monitored. The eyes were protected with contact lenses, stabilized by suturing to eye rings, and focused on a tangent screen 57 cm from the dog's eyes. A craniotomy was made over the thalamus. Low-impedance tungsten microelectrodes (1 MΩ) were used to record from visually responsive cells in the LGN. The electrodes were advanced vertically into the LGN. Typically, 3–6 penetrations yielded long sequences of visual receptive fields. The position of the area centralis and the meridia were estimated with reference to the plotted position of the optic disks (20° central and 5° inferior). Whenever possible, receptive fields were plotted every 100–200 μm along penetrations through the LGN, and small electrolytic lesions were made to facilitate track identification and reconstruction. At the conclusion of the experiment, animals were given an overdose of pentobarbital (30–40 mg kg^{-1}; i.v.) and perfused transcardially with fixative. The brain, eyes and optic nerves were dissected free from the cranium. Brains were sectioned at 50 μm on a freezing microtome and stained with cresyl violet.

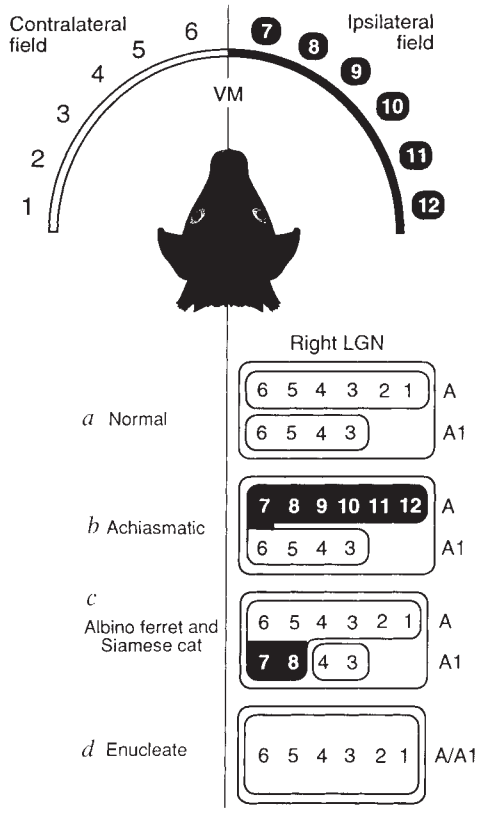

FIG. 4 Simple schemes of lamination and the representation of visual space in layers A and A1 of the carnivore LGN. The horizontal meridian of the visual field is represented as a numbered semicircle. In the schematics of the right LGN, dark areas represent abnormal representations of the ipsilateral visual field. *a*, The pattern of lamination, retinotopy and visuotopy of normal dogs is comparable to that seen in other carnivores. The area of contralateral visual space viewed by the two eyes is aligned in precise register across layers A and A1 (ref. 1). *b*, The achiasmatic pattern in which the entire ipsilateral hemifield (numbers in dark blocks) is represented in layer A. These ipsilateral fields in layer A are out of register with the contralateral fields in layer A1. *c*, The common pattern in the LGN of Siamese cat and albino ferret, in which the lamination abnormality affects only the medial part of layer A1 (refs 14–17). *d*, The pattern following prenatal or early postnatal enucleation in carnivores[17,19]. Contralateral to the remaining eye, layers A and A1 have formed a composite layer A/A1.

with respect to that in normal dogs and with respect to that in the relatively normal layer A1 of mutant dogs. This results in mirror-image maps in layers A and A1 that cover the entire visual space and which are congruent only at the representation of the vertical meridian (Fig. 4*b*). It is possible that the vertical meridian is duplicated in A and A1 and that these layers contain independent, but fused maps. It is also possible that there is a single map wrapped around on itself at the vertical meridian representation. The well-ordered mirror-image maps in the mutant LGN indicate that genes that control the crossing of retinal axons at the chiasm differ from those that regulate the formation of maps in the LGN.

Despite its monocular innervation, three relatively normal characteristics of the mutant LGN are surprising. It is not obvious why the so-called binocular and monocular segment of LGN layers would be preserved in the entirely monocular LGN of the mutants (Fig. 2), why nearly symmetrical receptive field positions would be recorded across the A/A1 border (Fig. 3), or why the point at which layers A and A1 are fused would correspond to the vertical meridian. All three features can be explained if positional specificity between retinal axons and LGN cells and layers is rigidly preserved, despite the misrouting of nasal axons at the chiasm. The preservation of target recognition in mutants most probably reflects a fixed chemoaffinity between subsets of retinal axons and LGN neurons[22–24]. This mutation shows that the selection of a target site in the LGN is not controlled by the eye of origin (namely, ipsilateral or contralateral), but rather that the critical factors are the retinal position from which axons originate and positional specificity within the LGN. □

Received 15 September; accepted 13 December 1993.

1. Kaas, J. H., Guillery, R. W. & Allman, J. M. *Brain Behav. Evol.* **6,** 253–299 (1972).
2. Williams, R. W., Garraghty, P. E. & Goldowitz, D. *Soc. Neurosci. Abstr.* **17,** 187 (1991).
3. Hogan, D., Garraghty, P. E. & Williams, R. W. *Soc. Neurosci. Abstr.* **19,** 524 (1993).
4. Dell'Osso, L. F. *Curr. Neuro. Ophthalmol.* **1,** 139–172 (1988).
5. Williams, R. W. & Dell'Osso, L. F. *Invest. Ophthalmol. Vis. Sci.* **34,** 1125 (1993).
6. Rioch, D. M. *J. comp. Neurol.* **49,** 1–119 (1929).
7. Sanderson, K. J. *J. comp. Neurol.* **143,** 101–118 (1971).
8. Apkarian, P., Bour, L. & Barth, P. G. *Eur. J. Neurosci.* (in the press).
9. Guillery, R. W. *Trends Neurosci.* **9,** 364–367 (1986).
10. Stone, J., Campion, J. E. & Leicester, J. *J. comp. Neurol.* **180,** 783–798 (1978).
11. Cooper, M. L. & Pettigrew, J. D. *J. comp. Neurol.* **187,** 313–348 (1979).
12. Leventhal, A. G. & Creel, D. J. *J. Neurosci.* **5,** 795–807 (1985).
13. Balkema, G. W. & Dräger, U. C. *Vis. Neurosci.* **4,** 595–604 (1990).
14. Hubel, D. H. & Wiesel, T. N. *J. Physiol.* **218,** 33–62 (1971).
15. Guillery, R. W. & Kaas, J. H. *J. comp. Neurol.* **143,** 73–100 (1971).
16. Huang, K. & Guillery, R. W. *Devl Brain Res.* **20,** 213–220 (1985).
17. Guillery, R. W., Lamantia, S. A., Robson, J. A. & Huang, K. *J. Neurosci.* **5,** 1370–1379 (1985).
18. Rakic, P. *Science* **214,** 928–931 (1981).
19. Chalupa, L. M. & Williams, R. W. *Hum. Neurobiol.* **3,** 103–107 (1984).
20. Garraghty, P. E., Shatz, C. J. & Sur, M. *Vis. Neurosci.* **1,** 93–102 (1988).
21. Berman, N. & Cynader, M. *J. Physiol.* **224,** 363–389 (1972).
22. Walsh, C., Polley, E. H., Hickey, T. L. & Guillery, R. W. *Nature* **302,** 611–614 (1983).
23. Sperry, R. W. *Proc. natn. Acad. Sci. U.S.A.* **50,** 703–710 (1963).
24. Bonhoeffer, F. & Huf, F. *Nature* **315,** 409–410 (1985).

ACKNOWLEDGEMENTS. This work was supported by the NIH and the National Eye Institute. We thank A. de LaHunta, J. Cummings and M. Young for their help in starting this project; B. Belton and T. Mandrell for animal care; T. Kimble for technical help; J. Kaas for facilities at Vanderbilt University; and N. Berman, E. Geisert, L. Dell'Osso and D. Goldowitz for discussion.

Rhodopsin mutation G90D and a molecular mechanism for congenital night blindness

Vikram R. Rao, George B. Cohen & Daniel D. Oprian

Graduate Department of Biochemistry, Brandeis University, Waltham, Massachusetts 02254, USA

MUTATIONS in the gene for the visual pigment rhodopsin cause retinitis pigmentosa (RP) and congenital night blindness[1–7]. Inheritance of the diseases is generally autosomal dominant and about 40 different rhodopsin mutations have been documented. Although the cell death and retinal degeneration associated with RP have been suggested to result from improper folding and accumulation of the mutant proteins in rod photoreceptor cells[8], this may not account for the disease in all cases. For example, RP mutations at Lys 296, site of Schiff base linkage to the retinal chromophore, result in constitutive activation of the protein *in vitro*[9–11]; that is, the mutants can catalytically activate the G protein transducin in the absence of chromophore and in the absence of light. Similarly, mutation of Ala 292 → Glu activates opsin *in vitro* and causes night blindness[7]. We show here that the mutation Gly 90 → Asp (G90D) in the second transmembrane segment of rhodopsin, which causes congenital night blindness[12], also constitutively activates opsin. Furthermore, we show that Asp 90 can substitute for the Schiff base counterion, Glu 113, which is located in the third transmembrane segment of the protein. This demonstrates the proximity of Asp 90 and Lys 296 in the three-dimensional structure of rhodopsin and suggests that the constitutively activating mutations operate by a common molecular mechanism, disrupting a salt bridge between Lys 296 and the Schiff base counterion, Glu 113.

Figure 1 shows that the Gly 90→Asp (G90D) mutant rhodop-